Hindawi Publishing Corporation
International Journal of Photoenergy
Volume 2015, Article ID 537538, 10 pages
http://dx.doi.org/10.1155/2015/537538

Research Article

Electrical and Thermal Performance Analysis for a Highly Concentrating Photovoltaic/Thermal System

Ning Xu, Jie Ji, Wei Sun, Wenzhu Huang, and Zhuling Jin

Department of Thermal Science and Energy Engineering, University of Science and Technology of China, No. 96 Jinzhai Road, Hefei, Anhui 230027, China

Correspondence should be addressed to Jie Ji; jijie@ustc.edu.cn

Received 9 July 2015; Revised 11 October 2015; Accepted 12 October 2015

Academic Editor: Elias Stathatos

A 30 kW highly concentrating photovoltaic/thermal (HCPV/T) system has been constructed and tested outdoors. The HCPV/T system consists of 32 modules, each of which consists of point-focus Fresnel lens and triple-junction solar cells with a geometric concentrating ratio of 1090x. The modules are connected to produce both electrical and thermal energy. Performance analysis has been conducted from the viewpoint of thermodynamics. The experimental results show that highest photovoltaic efficiency of 30% and instantaneous thermal efficiency of 30% can be achieved at the same time, which means the total solar energy conversion efficiency of the HCPV/T system is higher than 60%. The photovoltaic efficiency increases with direct irradiance when the direct irradiance is below 580 W/m^2, but it remains nearly unchanged when the direct irradiation is higher than 580 W/m^2. The instantaneous thermal efficiency decreases during water heating process. However, the electrical performance of the system is not affected obviously by water temperature. Highest exergetic efficiency of 35.4% can be produced by the HCPV/T system. The exergetic efficiency is mainly affected by irradiation level, which is similar to the characteristics of photovoltaic performance.

1. Introduction

Concentrator photovoltaic technology has been developed for over 30 years since the first modern PV concentrator was made at Sandia National Laboratories. Highly concentrating photovoltaic (HCPV) could be an important avenue for solar electricity to become economical in mass production [1]. The general idea of concentrator photovoltaic is to use optics to focus sunlight on a small receiving solar cell. Therefore, the cell area in the focus of the concentrator can be reduced by the concentration ratio ($C > 300$ for HCPV systems). Consequently, this reduction allows the utilization of expensive but highly efficient multijunction solar cells in an economical manner. The efficiency of multijunction solar cells is reported to be higher than 40% [2–4]. On the CPV module level, photovoltaic above 30% has been reported [5–7].

CPV is developing very fast, and more and more researchers and entrepreneurs are joining in this field. Substantial CPV plants and demonstration systems have been established in China, Australia, Spain, and Japan and elsewhere. Compared with other high concentrators, Fresnel lens recently has been one of the best choices because of its advantages such as small volume, light-weight, and mass production with low cost as well as effectively increasing the energy density. Araki et al. [8] present a 30 kW concentrator photovoltaic system using dome-shaped Fresnel lenses. Its photovoltaic efficiency can reach 25.8%. Xie et al. [9] give a review on concentrated solar energy applications using Fresnel lenses in the last two decades, the highest photovoltaic conversion efficiency based on imaging Fresnel lens and nonimaging Fresnel lens is reported as over 30% and 31.5 ± 1.7%, respectively. Among the existing point-focus Fresnel CPV systems, almost all the modules are passively cooled. One point of view [10] believes that passive cooling could work well for single-cell geometries for flux levels as high as 1000x suns, because there is large area available for heat sinking. However, the fact is that a large part of the already collected solar energy is dissipated as heat to the environment for modules with passive cooling design.

An active thermal circulation with coolant fluid can enable heat transfer from the central receiver to a thermal load so that the dissipated heat is collected as usable energy. Hence, the total solar energy conversion efficiency

Figure 1: Photograph of the 30 kW HCPV/T system.

is significantly increased. This thermal energy can be used directly for domestic or industrial heating. Besides, some poly generation approaches can also generate either cooling power or drinking water from the heat using solar cooling and air conditioning [11–13] or solar desalination [14, 15] technologies. Therefore, the integration of PV/T system and CPV system with point-focus Fresnel lens deserves to be respected. Unfortunately, although researches on PV/T technology, highly concentrators, multijunction solar cells, and point-focus Fresnel photovoltaic system with passive cooling methods have been carried out for years; the attempt to combine them in a hybrid system is rarely reported, especially on array level.

In this paper, a novel highly concentrating photovoltaic/thermal (HCPV/T) system based on point-focus Fresnel lens is originally proposed. Both electrical and thermal power can be cogenerated by this system. The system whose overall peak power is 30 kW is established and tested outdoors. Both electrical and thermal performance analyses are conducted from the point of view of thermodynamics. Besides, a detailed description for the main components of the system and their principles is also introduced in this paper. This work is developed aiming to supply a reference or guidance on system design and performance analysis for similar attempts and projects.

2. Description of the HCPV/T System

2.1. Overview of the 30 kW HCPV/T System. The arrangement of the 30 kW HCPV/T system is shown in Figure 1. The system is located in Huainan (32.37°N 116.59°E), Anhui Province, China. It mainly consists of 32 point-focus Fresnel modules which are mounted on a dual-axis tracking structure, as shown in Figure 1. The HCPV/T array has two strings, each of which consists of 16 modules connected in series. The array is connected to an inverter. The dual-axis tracking system ensures that the HCPV/T array tracks the sun accurately and the inverter helps to output electrical power at the maximum power point. Thanks to specific design of the receiver, dissipated heat on the receiver is collected by circulating water which flows through the modules, the pipelines, the pump, and the water tank. Under operating condition, photovoltaic power is parallel in the grid and water in the storage tank is heated. In this way, solar energy is converted to both electrical energy and thermal energy.

Table 1: Typical electrical characteristic of the HCPV/T module.

Parameter	Variable	Value
Maximum power	P_m	402 W ± 5%
Voltage at P_m	V_m	38.3 V
Current at P_m	I_m	10.5 A
Open circuit voltage	V_{OC}	45.2 V
Short circuit current	I_{SC}	11.1 A

2.2. Design of the HCPV/T Module. A typical structure of the HCPV/T module used in this system is depicted in Figure 2. There are 15 point-focus Fresnel lenses and 15 CPV/T components in a single module. The Fresnel lens and CPV/T components are mounted one by one on the aluminum frame. High efficiency InGaP/GaAs/Ge solar cells whose photovoltaic efficiency is 31.4% (AM1.5D, 25°C) under 1x sun are adopted in this system. Each cell is laminated on an aluminum heat-sink with tube formulated directly on the rear side. On the top of the solar cell, a secondary optical prism is pasted by optical silicone. The schematic and photograph of a CPV/T component are shown in Figure 3. The heat-sink is designed with a structure of axis grooved tube. The solar cells are allowed to operate at highest temperature of 90°C for a short period. It has been proved that this kind of structure can guarantee that the solar cells operate safely based on our previous work [16]. Incident sunlight is refracted by Fresnel lens and then by optical prism to distribute uniform irradiance on solar cell. All the 15 solar cells are connected in series and adjacent tubes are connected by pipes. The electrical characteristic for the module offered by the manufacturer is listed in Table 1. They are achieved by indoor testing under steady condition (DNI 900 W/m^2, 20°C, 4 m/s). As the areas of each Fresnel lens and solar cell are 330.2 × 330.2 mm^2 and 10 × 10 mm^2, respectively, the geometric concentration ratio of the module is 1090x. With respect to the optical loss in the concentration process, the module can achieve an optical concentration ratio of 952x.

2.3. Dual-Axis Tracking System. Point-focus lens concentrator requires that the module is always pointed at the sun so that the concentrated light falls precisely on the cell. A dual-axis tracking system with roll-tilt configuration is adopted, as shown in Figure 4. Although this kind of structure contains more rotating bearings and linkages, the wind loads on drive components are considerably reduced. The roll axis is placed in a northsouth direction, as this minimizes shadowing by adjacent modules along the roll axis and further minimizes space between them. A couple of light sensors are installed in the middle of the tracking structure. The sensor is essentially composed of a pair of photodiodes and a shading device which casts a different shade on these photodiodes, thereby generating different photocurrents whenever it is not aligned with the local sun vector. The sensors are mounted with the same angle that the module tilts and one per tracking axis. The tracking controller works on a two-stage basis, first coarsely aiming based on sun-ephemeris computed coordinates, followed by fine pointing using the light sensors.

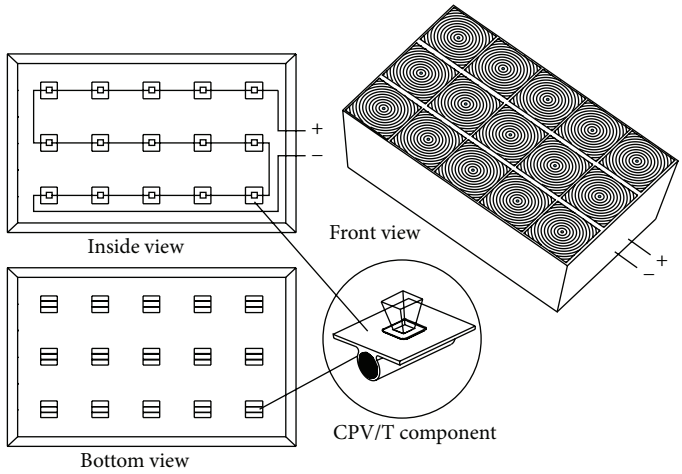

Figure 2: Schematic of the HCPV/T module based on point-focus Fresnel lens.

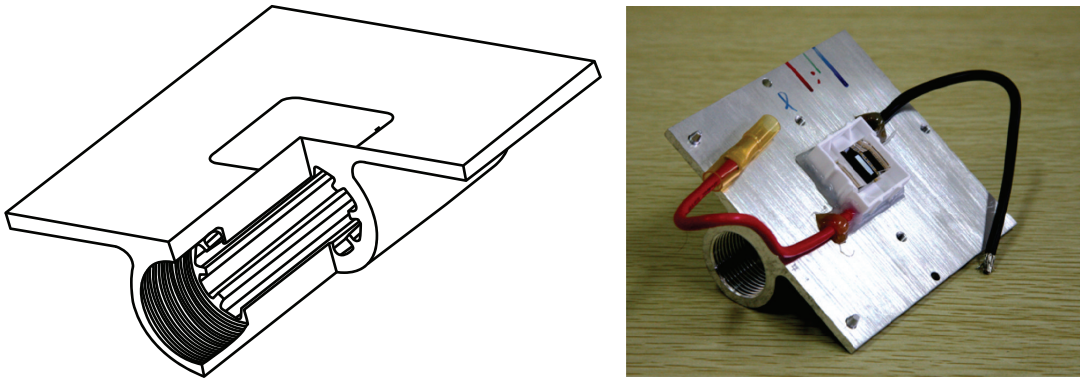

Figure 3: Schematic and photograph of a CPV/T component with grooved tube.

Figure 4: Photograph of the dual-axis tracking system.

In this system, the angle of incidence remains within a range of 0.3° with the help of the tracking system.

2.4. Water Circulation System. Figure 5 shows the schematic of the water circulation system. Water is pumped from the bottom of the storage tank and flows through the tubes below the heat-sinks. Heated water flows back to the tank. Every 60 heat-sink tubes of modules which are mounted on the same tilt axis are connected in series by pipes. This arrangement divides the water circulation system into eight branches and it also reduces mass flow discrepancy due to reversed return water circulation. At the inlet of main pipeline, a valve and a flowmeter are installed to control and measure the water flow rate, respectively. Two pressure gauges are installed at the inlet and outlet of the main pipeline, respectively. All pipes and heat-sink tubes are insulated by insulation cotton with a thickness of 15 mm. The volume of the tank in this system is 1000 L. Temperature measurement locations are also shown in Figure 5. Eight temperature measuring points are arranged uniformly in the water storage tank to eliminate the measurement error caused by water stratification.

2.5. Data Acquisition System. In the data acquisition system, temperature is measured by T-type thermocouples; direct normal irradiance (DNI) is measured by a pyrheliometer. Both temperature and DNI are recorded by a data logger (HIOKI LR8402-21) at an interval of 10 s. Pressure and water flow rate are also recorded. An inverter is used to measure and record the electrical power output of the HCPV/T modules. The electrical data is recorded every 5 minutes by the inverter. The details of all the measurement instruments are listed in Table 2.

3. Mathematical Model

3.1. Energy Balance Model. As stated before, both electrical and thermal energy are converted from solar energy by the

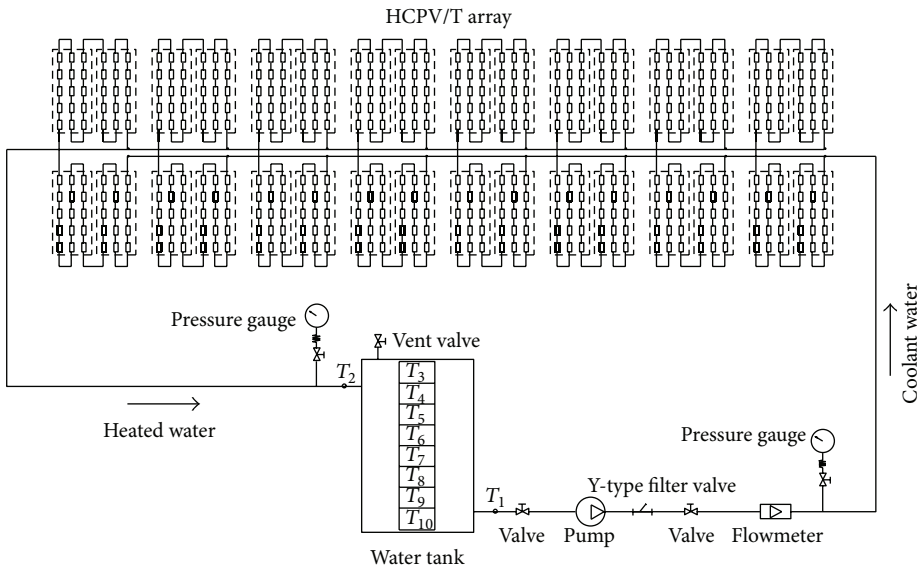

Figure 5: Schematic of water circulation and measuring point positions.

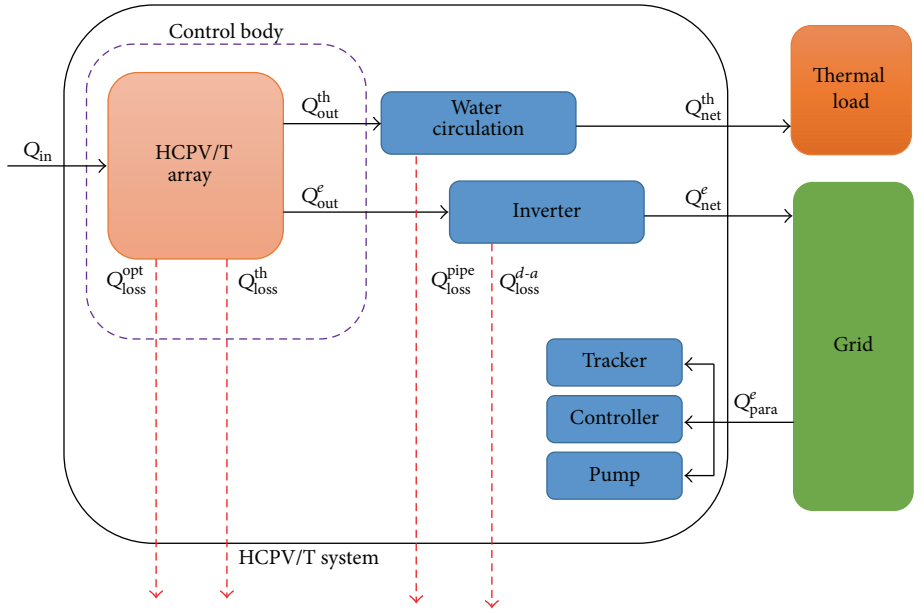

Figure 6: Schematic of the energy balance of a HCPV/T system.

Table 2: Characteristics of sensors and measurement instruments.

Device	Accuracy	Specification
Thermocouple	±0.2°C	T-type
Pyrheliometer	2%	TBS 2-2
Data logger		HIOKI LR8402-21
Flow rate	2%	LXS-40E
Inverter	3%	Guanya GSG-100KTT-TV

HCPV/T array. In this system, power output is tapped into the grid by an inverter directly and thermal output is collected without secondary heat exchange. Considering the energy losses caused by optical, electrical, and thermal reasons, the schematic drawing of the energy balance for the HCPV/T system is illustrated in Figure 6.

Based on the first law of thermodynamics, the general energy balance for the HCPV/T array can be expressed as

$$Q_{in} = Q^{e}_{out} + Q^{th}_{out} + Q^{opt}_{loss} + Q^{th}_{loss}, \quad (1)$$

where Q_{in} is the total incoming radiation power on all modules, Q^{e}_{out} is the photovoltaic output by the array, and Q^{th}_{out}

is thermal output at the same time. Calculations for them are illustrated by

$$Q_{\text{in}} = G_d A_m N_s N_p, \tag{2}$$

$$Q_{\text{out}}^{\text{th}} = c_p \dot{m} \left(T_{w,o} - T_{w,i}\right). \tag{3}$$

In (2), G_d is the incident beam radiation on the array, namely, the direct normal irradiance. A_m is the total Fresnel lens area of a single module. N_s is the number of modules in a series and N_p is the number of branches of the array. In (3), c_p is the specific heat of water, $\dot{m}$ is the total mass flow rate, and $T_{w,i}$ and $T_{w,o}$ are the inlet temperature and outlet temperature in the circulation, respectively.

In (1), $Q_{\text{loss}}^{\text{opt}}$ is the optical loss and it can be derived from (4). The optical efficiency η_{opt} considers optical losses caused by both Fresnel lens and prims; thereby it is the dot product of their transmittance, as shown in (5):

$$Q_{\text{loss}}^{\text{opt}} = Q_{\text{in}} \left(1 - \eta_{\text{opt}}\right), \tag{4}$$

$$\eta_{\text{opt}} = \tau_{\text{Fresnel}} \tau_{\text{prism}}. \tag{5}$$

The last part in (1), namely, $Q_{\text{loss}}^{\text{th}}$, is the thermal loss of the array caused by heat convection and radiation to the ambient. It is difficult to be calculated accurately. However, this part contributes insignificantly when evaluating the performance of the system.

It is should be emphasized that in an integrated system some parasitic power consumption from components inevitably exists. On the other hand, some energy losses such as thermal loss from pipes to the ambient are unavoidable even if the design is optimized. On account of these power consumption and losses, the net power generated by the HCPV/T system can be defined as

$$Q_{\text{net}}^{e} = Q_{\text{out}}^{e} - Q_{\text{loss}}^{d\text{-}a} - Q_{\text{para}}^{e}, \tag{6}$$

$$Q_{\text{net}}^{\text{th}} = Q_{\text{out}}^{\text{th}} - Q_{\text{loss}}^{\text{pipe}}. \tag{7}$$

In (6), Q_{net}^{e} is the net electrical power supplied by the system; $Q_{\text{loss}}^{d\text{-}a}$ is the energy loss due to inversion and grid connection. Q_{para}^{e} is parasitic power consumption which includes power dissipation from tracker, controller and pump. In (7), $Q_{\text{loss}}^{\text{pipe}}$ defines the heat loss from the pipes and storage tank. Because all the pipes and tank are thermally insulated perfectly, this part can usually be neglected.

3.2. First-Law Efficiency of Thermodynamics. Instantaneous efficiency is widely used to evaluate PV/T systems. The photovoltaic efficiency represents the ability of the HCPV/T array to convert solar energy to electrical energy. It is obtained by

$$\eta_{\text{PV}} = \frac{Q_{\text{out}}^{e}}{Q_{\text{in}}} = \frac{Q_{\text{out}}^{e}}{G_d A_m N_s N_p}. \tag{8}$$

The instantaneous thermal efficiency of the HCPV/T array is defined by (9), which reflects the heat conversion capability of the array:

$$\eta_{\text{th}} = \frac{Q_{\text{out}}^{\text{th}}}{Q_{\text{in}}} = \frac{c_p \dot{m} \left(T_{w,o} - T_{w,i}\right)}{G_d A_m N_s N_p}. \tag{9}$$

From the first-law of thermodynamics, the overall performance of a PV/T system can be evaluated by the energetic (first-law) efficiency η_{PVT}. It is widely used in previous studies [17, 18]. The first-law efficiency is defined as

$$\eta_{\text{PVT}} = \eta_{\text{PV}} + \eta_{\text{th}}. \tag{10}$$

3.3. Second-Law Efficiency of Thermodynamics. Although the first-law efficiency reveals the overall performance of a PV/T system directly, it ignores the difference between thermal energy and electrical output produced by a module in "quality," even if they are the same in "quantity" and measurable by the same physical unit. In fact, thermal energy cannot produce work until a temperature difference exists between a high temperature heat source and a low-temperature heat-sink, while electrical energy can completely transform into work irrespective of the environment. In other words, the second-law efficiency, namely, the exergetic efficiency, offers a qualitative and standardized evaluation of the overall performance of a PV/T system. Exergy is simply the available energy obtained by subtracting the unavailable energy from the total energy and is equivalent to the work transformable.

According to the work conducted by Fujisawa and Tani [19], the second-law efficiency of a PV/T system is expressed as (11). This definition is based on the assumption that the initial temperature of the fluid medium is equal to the ambient temperature:

$$\varepsilon_{\text{PVT}} = \varepsilon_{\text{PV}} + \varepsilon_{\text{th}} = \eta_{\text{PV}} + \left(1 - \frac{T_a}{T_w}\right) \eta_{\text{th}}, \tag{11}$$

where ε_{PV} and ε_{th} are the exergetic efficiency of PV array and thermal collectors, respectively. T_a is the ambient temperature and T_w is the water temperature which can be calculated by

$$T_w = \frac{\left(T_{w,i} + T_{w,o}\right)}{2}. \tag{12}$$

In (11), the calculation of the exergy of solar radiation is not considered. Instead, the energy of radiation is taken as the exergy of radiation directly. Exergetic efficiency is the ratio of total exergy output to total exergy input [20]. Therefore, the exergetic efficiency can be defined as

$$\varepsilon_{\text{PVT}} = \frac{\text{Ex}_{\text{PV}} + \text{Ex}_{\text{th}}}{\text{Ex}_{\text{in}}} = \varepsilon_{\text{PV}} + \varepsilon_{\text{th}}, \tag{13}$$

where Ex_{PV} and Ex_{th} are the electrical exergy output and thermal exergy output of the array, respectively. Ex_{in} is the

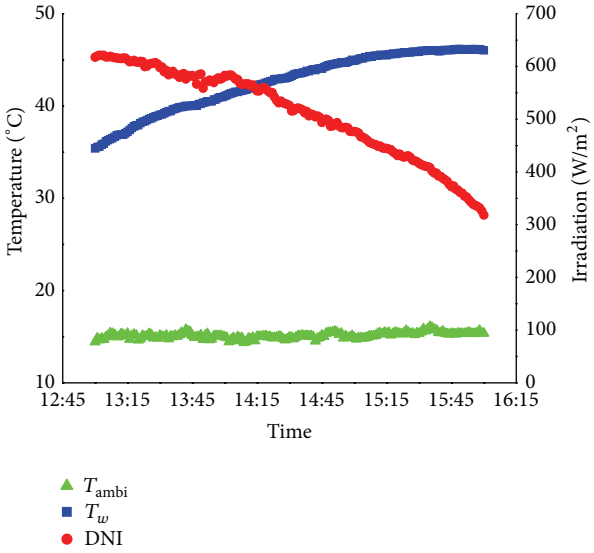

Figure 7: Environmental parameters in the testing period.

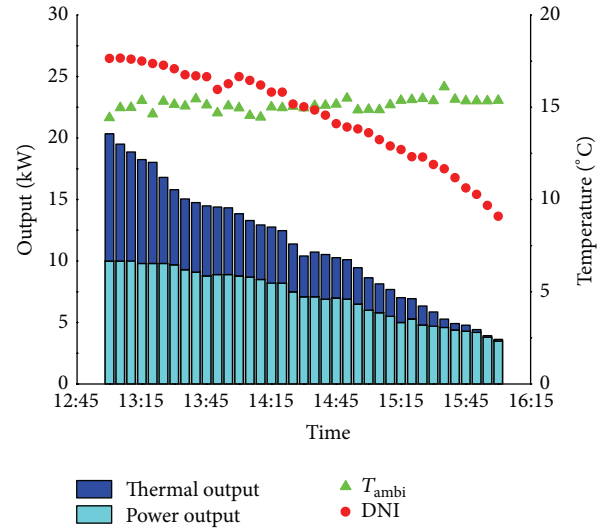

Figure 8: Photovoltaic and thermal output of the HCPV/T system in the testing period.

exergy input of solar radiation. The exergy outputs are related to the energy outputs as follows:

$$\begin{aligned} \mathrm{Ex}_{\mathrm{PV}} &= Q^{e}_{\mathrm{out}}, \\ \mathrm{Ex}_{\mathrm{th}} &= \left(1 - \frac{T_a}{T_w}\right) Q^{\mathrm{th}}_{\mathrm{out}}. \end{aligned} \tag{14}$$

There are different methods to determine the exergy of radiation in evaluating the performance of PV/T system when using the exergy method. Among them, three most commonly used calculation methods are summarized by Chow et al. [17]; namely,

$$\mathrm{Ex}_{\mathrm{in}} = \left[1 + \frac{1}{3}\left(\frac{T_a}{T_{\mathrm{sun}}}\right)^4 - \frac{4T_a}{3T_{\mathrm{sun}}}\right] Q_{\mathrm{in}}, \tag{15}$$

$$\mathrm{Ex}_{\mathrm{in}} = \left[1 - \frac{4T_a}{3T_{\mathrm{sun}}}\right] Q_{\mathrm{in}}, \tag{16}$$

$$\mathrm{Ex}_{\mathrm{in}} = \left[1 - \frac{T_a}{T_{\mathrm{sun}}}\right] Q_{\mathrm{in}}, \tag{17}$$

where T_{sun} is the solar radiation temperature at 6000 K. Actually, the difference between results calculated by these three methods is less than 2%. In this study, (17) is adopted.

4. Results and Discussion

The experiment was firstly conducted on December, 2014. Figure 7 shows changes of meteorological parameters and temperature of water in storage tank from 13:00 to 16:00 in a testing day. As seen in Figure 7, the ambient temperature changes in a small range of 15~17°C, and the DNI changes within 300~650 W/m^2. 1000 L water is heated from 35°C to 47°C in three hours. Water flow rate is controlled at 2.8 m^3/h which means the flow rate in each branch is nearly at 0.34 m^3/h. This flow rate makes the flow in tubes behavior

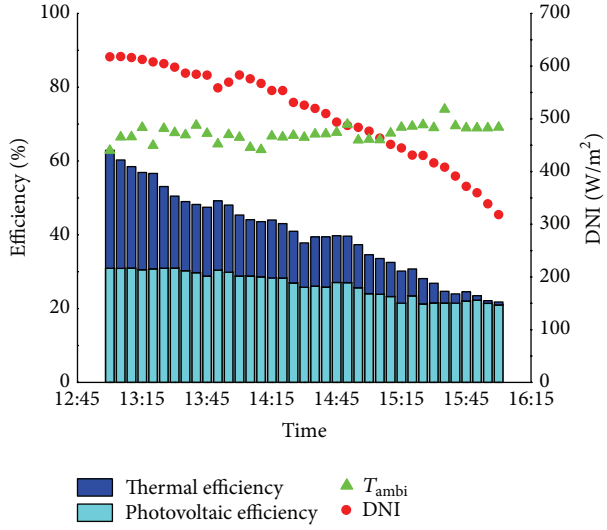

Figure 9: Efficiency characteristics of the HCPV/T system in the testing day.

a turbulent flow, thereby enhancing the heat convection effectiveness.

Figures 8 and 9 illustrate the output and efficiency of the HCPV/T system during the testing period, respectively. It can be seen in Figure 8 that the total output of the system exceeds 20 kW. Both power output and thermal output decrease as DNI decreases and water heated. Considering that the maximum DNI in the selected data is not higher than 650 W/m^2, more power can be obtained when the DNI level is higher. On the other hand, the heat collection capability can be definitely improved with a lower initial water temperature. Figure 9 depicts both photovoltaic efficiency and thermal efficiency changes in the testing period which can reflect the energy conversion effect directly. It is obvious that photovoltaic efficiency changes little with irradiation or water

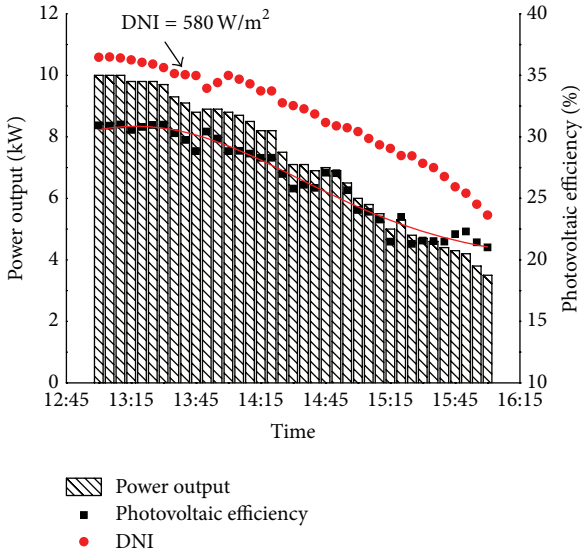

Figure 10: Photovoltaic performance of the HCPV/T array.

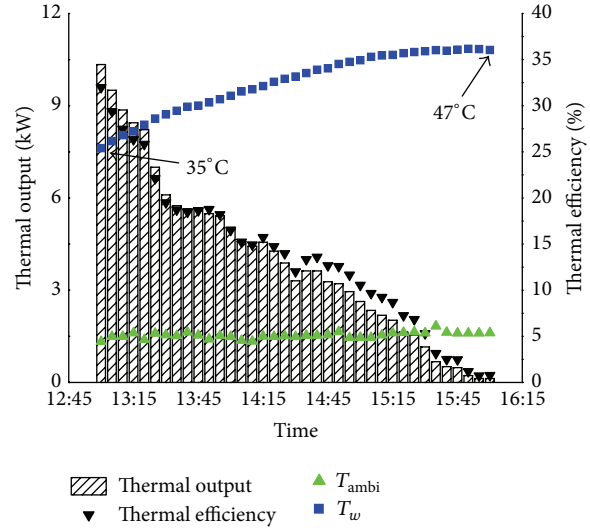

Figure 11: Thermal performance of the HCPV/T array.

temperature. However, thermal efficiency reduces quickly because of increasing water temperature and decreasing irradiation. Combining results revealed by Figures 8 and 9, it is conspicuous that higher power and thermal output can be obtained if the irradiation level is higher or water temperature is lower. Based on the electrical parameters of module and thermal characteristic of the system, it can be estimated that the total peak output generated by the system can be over 30 kW.

To investigate the photovoltaic characteristics of the system in particular, the relationship between power output, photovoltaic efficiency, and DNI is constructed in Figure 10. It can be found that the photovoltaic efficiency changes within 20~30%. Besides, the photovoltaic efficiency of the system increases with DNI when DNI is below 580 W/m^2 but remains nearly unchanged when DNI is higher than 580 W/m^2. This sign explains why the power output decreases more quickly when the irradiation is at a low level. It also indicates that the HCPV/T system will maintain a relatively high photovoltaic efficiency if it is arranged at a location with high direct irradiation level.

Figure 11 shows the thermal characteristics of the HCPV/T system. The thermal efficiency reduces because of the weaker heat capture ability resulting from higher water temperature and less energy input. In consequence, the thermal output decreases accordingly. It can be seen that thermal efficiency drops nearly to zero after 16:00, which means water circulation cannot collect heat positively. This gives signs that water cannot be heated sequentially under the current condition and the measure we should take is to stop pumping. It can be concluded that the thermal efficiency of the system will be higher than it is like currently if a larger tank is adopted because there is more low-temperature water to be heated up. However, the larger volume water may not be heated up to a relatively high temperature if the irradiation level is lower or the energy loss is higher, let alone the increasing cost of tank. It can be seen that water is heated up to 47°C. In fact, water with this grade of temperature can be used for domestic heating directly.

Performance of the HCPV/T array is compared with performance on the module level, which is investigated in our previous work [16]. The comparison is depicted in Figure 12. As to the selected data, water was heated from 35°C to 47°C, and the ambient temperature remained near 16°C without large fluctuation. The distinct difference exists in direct irradiation levels. It can be seen that at high irradiation level the HCPV/T array can obtain a higher photovoltaic efficiency than the module, but this difference is very small. This is mainly caused by measurement error due to different measuring instruments. Power output of the array is controlled by an inverter, while the module is measured by a photovoltaic analyzer. Even so, a photovoltaic efficiency of more than 28% can be obtained no matter on module level or array level. As to the thermal performance, thermal efficiency of the HCPV/T array is lower than that of module, and it decreases much faster than thermal efficiency of module. This is because there are longer and more complicated pipe routes in array compared to the module, and they will lead to larger heat loss.

The variation of overall efficiency of the HCPV/T system is shown in Figure 13. From the viewpoint of the first law of thermodynamics, highest overall efficiency of 62% can be obtained. It drops because of increasing water temperature and decreasing DNI. However, water temperature is found to play an insignificant role when the overall performance is viewed from the second law viewpoint. Highest exergetic efficiency of 35.4% can be produced by the HCPV/T system. The exergetic efficiency is mainly affected by irradiation level, which is similar to the characteristics of photovoltaic performance.

5. Conclusion

A 30 kW HCPV/T system based on the point-focus Fresnel lens is built and an outdoor experiment was performed

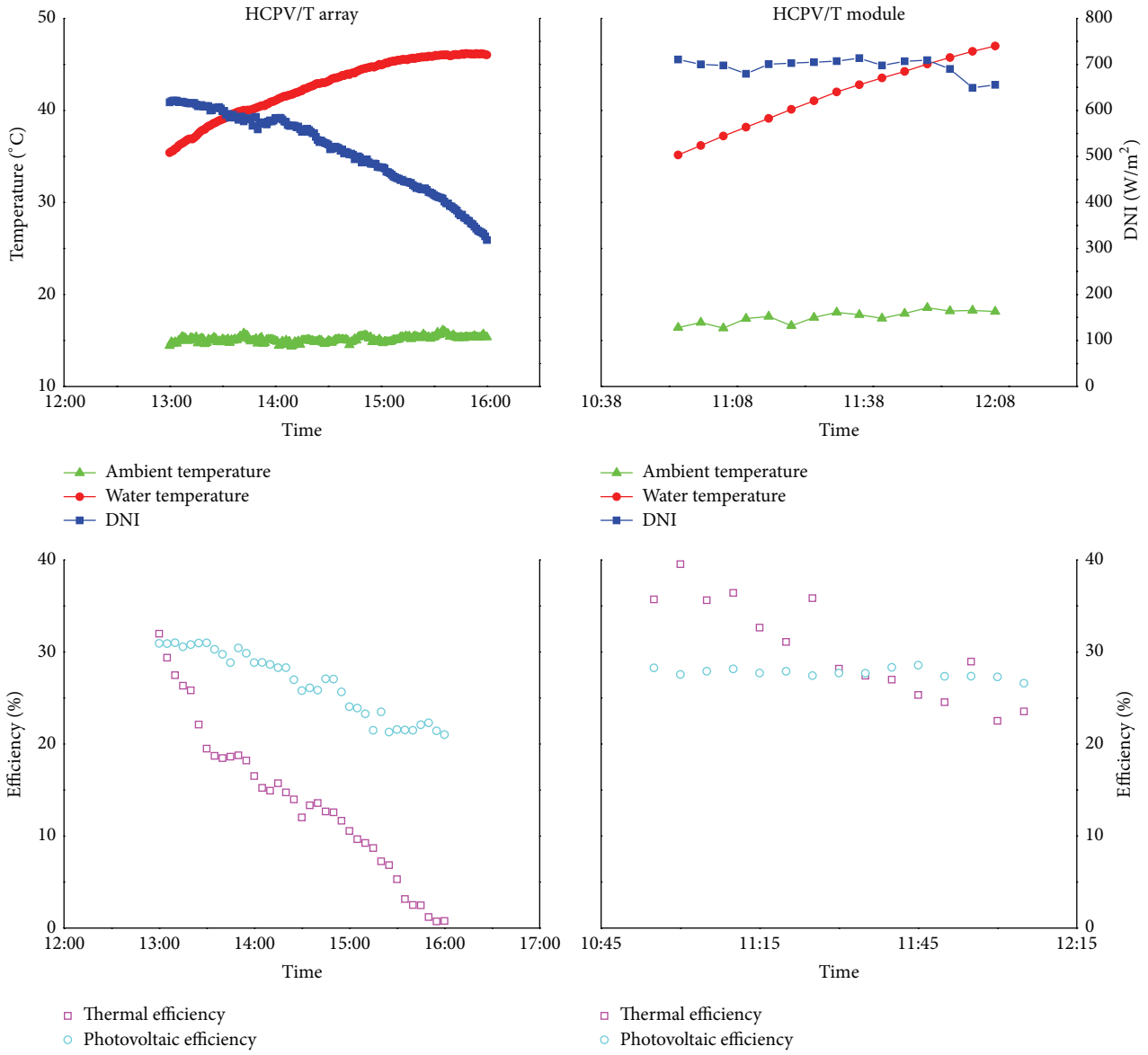

Figure 12: Comparison of performance between the HCPV/T array and a HCPV/T module.

in consecutive days. Outdoor performance of the system was also investigated based on periodical representative measurement data. Design principles and descriptions of each of several parts of the system are given in detail, aiming to present reference or guidance for similar attempts and projects. Performance analysis has been conducted from the viewpoint of thermodynamics with energetic analysis and exergetic analysis. The experimental results show that highest photovoltaic efficiency of 30% and instantaneous thermal efficiency of 30% could be achieved at the same time, which means the total solar energy conversion efficiency of the HCPV/T system is higher than 60%. The photovoltaic efficiency of the system increases with DNI when DNI level is below 580 W/m^2 but remains nearly unchanged when DNI is higher than 580 W/m^2. The instantaneous thermal efficiency decreases during water heating process because it strongly depends on water temperature as well as irradiation level. However, the electrical performance of the system is not affected obviously by the increase of water temperature. Highest exergetic efficiency of 35.4% can be produced by the HCPV/T system. The exergetic efficiency is mainly affected by irradiation level, which is similar to the characteristics of photovoltaic performance.

Nomenclature

Symbols

A: Area, m^2
c_p: Specific heat, J/(kg·K)
G_d: Direct normal irradiation, W/m^2
I: Current, A
$\dot{m}$: Mass flow rate, kg/s
N: Number of modules

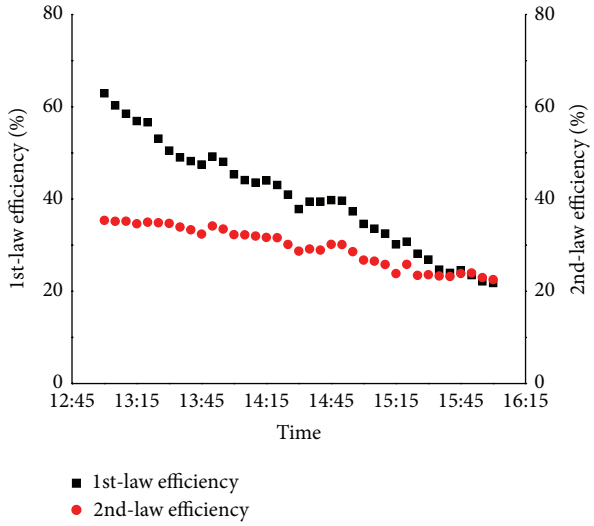

FIGURE 13: Variation of overall efficiency of the HCPV/T system.

Q: Energy, W
Ex: Exergy, W
T: Temperature, ˚C
V: Voltage, V.

Subscript/Superscript

d-a: DC to AC
e: Electrical
Fresnel: Fresnel lens
i: Inlet
in: Input
loss: Energy loss
m: Module
net: Net output
o: Outlet
opt: Optical
out: Output
p: In parallel
para: Parasitic
pipe: Pipe in circulation
prism: Optical prism
s: In series
th: Thermal
w: Water.

Greek Symbols

ε: Exergetic efficiency
η: Energetic efficiency
τ: Transmittance.

Conflict of Interests

The authors declare that there is no conflict of interests regarding the publication of this paper.

Acknowledgments

This work is supported by a grant from the National High Technology Research and Development Program of China (863 Program) (no. 2013AA050403) and Dongguan Innovative Research Team Program (no. 2014607101008).

References

[1] A. L. López and V. M. Andreev, *Concentrator Photovoltaics*, Springer, Berlin, Germany, 2010.

[2] S. Kurtz and J. Geisz, "Multijunction solar cells for conversion of concentrated sunlight to electricity," *Optics Express*, vol. 18, no. 9, pp. A73–A78, 2010.

[3] M. Yamaguchi, T. Takamoto, K. Araki, and N. Ekins-Daukes, "Multi-junction III-V solar cells: current status and future potential," *Solar Energy*, vol. 79, no. 1, pp. 78–85, 2005.

[4] F. Dimroth, M. Grave, P. Beutel et al., "Wafer bonded four-junction GaInP/GaAs//GaInAsP/GaInAs concentrator solar cells with 44.7% efficiency," *Progress in Photovoltaics: Research and Applications*, vol. 22, no. 3, pp. 277–282, 2014.

[5] K. Araki, H. Uozumi, T. Egami et al., "Development of concentrator modules with dome-shaped fresnel lenses and triple-junction concentrator cells," *Progress in Photovoltaics: Research and Applications*, vol. 13, no. 6, pp. 513–527, 2005.

[6] G. S. Kinsey, A. Nayak, M. Liu, and V. Garboushian, "Increasing power and energy in amonix CPV solar power plants," *IEEE Journal of Photovoltaics*, vol. 1, no. 2, pp. 213–218, 2011.

[7] S. van Riesen, A. Gombert, E. Gerster et al., "Concentrix Solar's progress in developing highly efficient modules," *AIP Conference Proceedings*, vol. 1407, p. 235, 2011.

[8] K. Araki, T. Yano, and Y. Kuroda, "30 kW concentrator photovoltaic system using dome-shaped Fresnel lenses," *Optics Express*, vol. 18, no. 1, pp. A53–A63, 2010.

[9] W. T. Xie, Y. J. Dai, R. Z. Wang, and K. Sumathy, "Concentrated solar energy applications using Fresnel lenses: a review," *Renewable and Sustainable Energy Reviews*, vol. 15, no. 6, pp. 2588–2606, 2011.

[10] A. Royne, C. J. Dey, and D. R. Mills, "Cooling of photovoltaic cells under concentrated illumination: a critical review," *Solar Energy Materials and Solar Cells*, vol. 86, no. 4, pp. 451–483, 2005.

[11] H.-M. Henning, "Solar assisted air conditioning of buildings—an overview," *Applied Thermal Engineering*, vol. 27, no. 10, pp. 1734–1749, 2007.

[12] C. A. Balaras, G. Grossman, H.-M. Henning et al., "Solar air conditioning in Europe—an overview," *Renewable and Sustainable Energy Reviews*, vol. 11, no. 2, pp. 299–314, 2007.

[13] G. Mittelman, A. Kribus, and A. Dayan, "Solar cooling with concentrating photovoltaic/thermal (CPVT) systems," *Energy Conversion and Management*, vol. 48, no. 9, pp. 2481–2490, 2007.

[14] J. Koschikowski, M. Wieghaus, and M. Rommel, "Membrane distillation for solar desalination," in *Seawater Desalination*, Green Energy and Technology, pp. 165–187, Springer, Berlin, Germany, 2009.

[15] G. Mittelman, A. Kribus, O. Mouchtar, and A. Dayan, "Water desalination with concentrating photovoltaic/thermal (CPVT) systems," *Solar Energy*, vol. 83, no. 8, pp. 1322–1334, 2009.

[16] N. Xu, J. Ji, W. Sun, L. Han, H. Chen, and Z. Jin, "Outdoor performance analysis of a 1090× point-focus Fresnel high concentrator photovoltaic/thermal system with triple-junction solar cells," *Energy Conversion and Management*, vol. 100, pp. 191–200, 2015.

[17] T. T. Chow, G. Pei, K. F. Fong, Z. Lin, A. L. S. Chan, and J. Ji, "Energy and exergy analysis of photovoltaic-thermal collector

with and without glass cover," *Applied Energy*, vol. 86, no. 3, pp. 310–316, 2009.

[18] J. Ji, J.-P. Lu, T.-T. Chow, W. He, and G. Pei, "A sensitivity study of a hybrid photovoltaic/thermal water-heating system with natural circulation," *Applied Energy*, vol. 84, no. 2, pp. 222–237, 2007.

[19] T. Fujisawa and T. Tani, "Annual exergy evaluation on photovoltaic-thermal hybrid collector," *Solar Energy Materials and Solar Cells*, vol. 47, no. 1–4, pp. 135–148, 1997.

[20] A. Hepbasli, "A key review on exergetic analysis and assessment of renewable energy resources for a sustainable future," *Renewable and Sustainable Energy Reviews*, vol. 12, no. 3, pp. 593–661, 2008.